JOURNAL OF AGRICULTURAL AND FOOD CHEMISTRY

ARTICLE

pubs.acs.org/JAFC

Determining Milk Isolated and Conjugated *trans*-Unsaturated Fatty Acids Using Fourier Transform Raman Spectroscopy

Ivan Stefanov,[†] Vincent Baeten,[‡] Ouissam Abbas,[‡] Ellen Colman,[†] Bruno Vlaeminck,[†] Bernard De Baets,[§] and Veerle Fievez*[,†]

[†]Laboratory for Animal Nutrition and Animal Product Quality (LANUPRO), Faculty of Bioscience Engineering, Ghent University, Proefhoevestraat 10, B-9090 Melle, Belgium

[‡]Food and Feed Quality Unit, Valorisation of Agricultural Products Department, Walloon Agricultural Research Centre, Chaussée de Namur, 24. B-5030 Gembloux, Belgium

[§]Department of Mathematical Modeling, Statistics and Bioinformatics, Faculty of Bioscience Engineering, Ghent University, Coupure links 653, B-9000 Ghent, Belgium

ABSTRACT: The feasibility of Raman spectroscopy in combination with partial least-squares (PLS) regression for the determination of individual or grouped *trans*-monounsaturated fatty acids (*trans*-MUFA) and conjugated linoleic acids (CLA) in milk fat is demonstrated using spectra obtained at two temperature conditions: room temperature and after freezing at −80 °C. The PLS results displayed capability for direct semiroutine quantification of several individual CLA (*cis*-9,*trans*-11 and *trans*-10,*cis*-12 C18:2) and *trans*-MUFA (*trans*-4−15 C18:1) in minor concentrations (below 1.0 g/100 g of milk fat). Calibration models were based on reference data cross-correlation or determined by specific scattering signals in the Raman spectra. Distinct bands for *trans*-MUFA (1674 cm^{-1}) and CLA (1653 cm^{-1}) from the *trans* isolated and *cis*,*trans* conjugated C═C bonds were identified, as well as original evidence for the temperature effect (new bands, peak shifts, and higher intensities) on the Raman spectra of fatty acid methyl ester and triacylglyceride standards, are supplied.

KEYWORDS: FT-Raman, spectroscopy, PLS, MSC, milk fat, *trans*-fatty acids, CLA

INTRODUCTION

Consumers have an increased awareness and concerns about the relationship between dairy food composition and human health. The nutritional value of milk is dependent on the amount of fatty acids (FAs) with important physiological functionalities. Positional isomers of conjugated linoleic acid (CLA) have been found to have both positive (*cis*-9,*trans*-11 C18:2 CLA inhibits carcinogenesis and reduces cardiovascular risk and inflammation) and adverse (*trans*-10,*cis*-12 C18:2 CLA may elevate the risk of developing diabetes) effects for human health.[1,2] Furthermore, *trans*-monounsaturated fatty acids (*trans*-MUFA) are linked to many cardiovascular detrimental effects, although recent reports indicate the benefit of higher doses of *trans*-11 C18:1, the precursor of rumenic acid in bioconversion via δ-9 dehydrogenation,[3,4] in the reduction of risk factors associated with heart disease, diabetes, and obesity in rats.[5]

Keeping in mind that *trans*-fatty acids (TFAs) might differ in their physiological effects, the subject of milk quality could be broadened to include health-related characteristics. Already, in several countries, such as Denmark in 2003 and later followed by Switzerland in 2008, scientific evidence of detrimental *trans*-MUFA effects have influenced implementation of legislation for banning the sale of various dairy and nondairy food products with a total TFA content higher than 2.0 g/100 g of the total fat.[6,7] Further, larger countries like Canada have not been able to agree on nationwide regulations, but individual provinces have taken different measures for regulating the sale of foods containing total TFAs: from strict labeling of all foods with a TFA content above 0.2 g per serving, to the less drastic step of limiting the total TFAs in dairy products to 5% of the total fat content.[8] Moreover, debates in the European Union are on the agenda, but the EU countries have not been able to achieve a common strategy since the release of the 2004 European Food Safety Authority scientific opinion report on TFAs.[9] Concurrently, different manufacturers have begun work on implementing various dietary programs for the decrease of milk saturated FAs and the increase in unsaturated FAs with an emphasis on CLA levels, which could also affect quantities of detrimental FAs.[10,11]

On the basis of the latter and taking into account the polar physiological effects of different TFAs, it is conspicuous that no common opinion with regard to the restrictions in foods could be achieved when looking at the collective amount of *trans*-FA; thus, the awareness for the determination of individual TFA constituents using a fast and cost-effective analytical method could emerge as a solution to help shape a common legislation in the near future. With this arises an important question of how to determine individual FAs in low concentrations using a fast and cost-effective analytical method.

Already, numerous gas liquid chromatography (GC) and high-performance liquid chromatography methods are available for the determination of FA profiles, but they require sample derivatization

Received: August 28, 2011
Accepted: November 15, 2011
Revised: November 11, 2011
Published: November 15, 2011

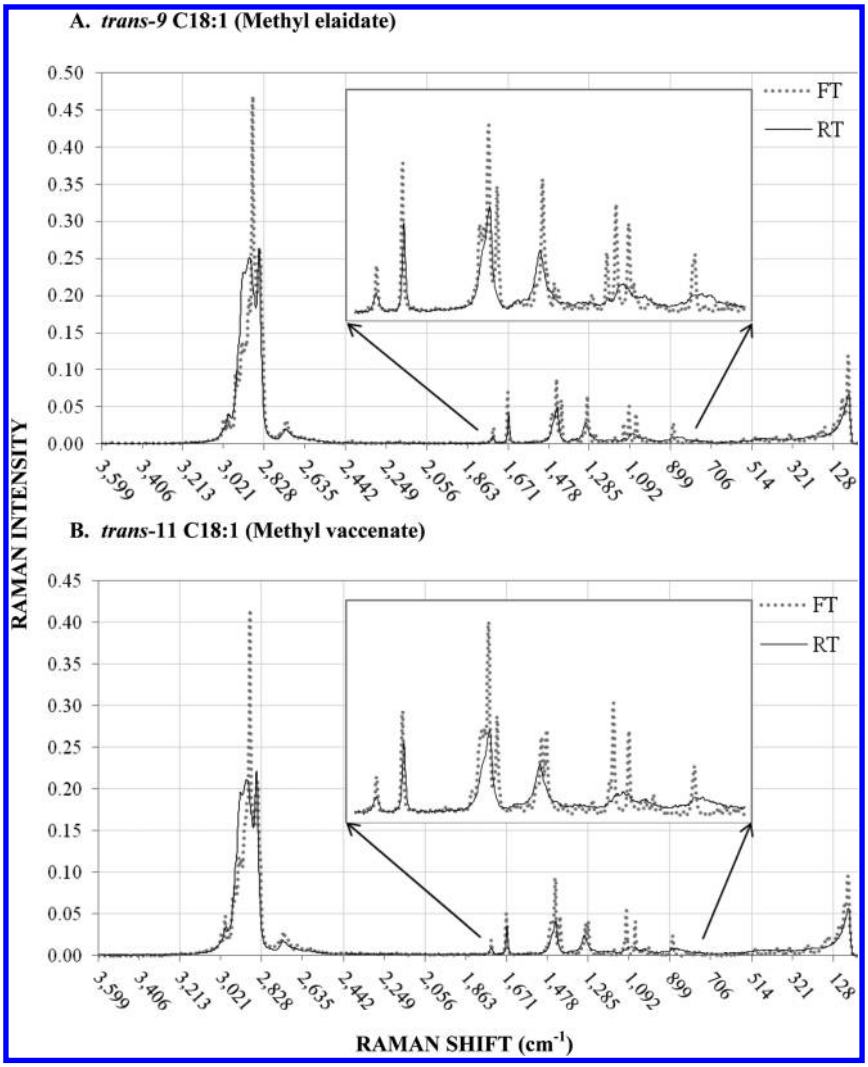

Figure 1. Multiplicative scatter-corrected (MSC) Raman spectra of solid (dotted, after freezing at −80 °C) vs RT (full) (A) *trans*-9 C18:1 and (B) *trans*-11 C18:1 pure FAMES [*x*-axis, wavenumbers (cm^{-1}); *y*-axis, scattering intensity].

and expert knowledge for chromatogram interpretation and thus are considerably slow and tedious and restrict determination to a limited number of samples per day.

Fourier transform infrared spectroscopy (FT-IR) transmission techniques have been successfully introduced in the quantification of isolated TFAs in various vegetable oils and fats[12−14] but have not been satisfactory with low concentration (<5.0 g/100 g of total fat) determinations in more complex matrices such as milk fat.[15,16] One of the reasons is that the C−H deformation band in the single and poly *trans* C═C bonds absorb in midinfrared (MIR) between 975 and 955 cm^{-1}; thus, the TFA absorption band appears in a high, sloping part of the spectrum and hinders estimations of FAs in low concentrations. Attenuated total reflectance infrared spectroscopy (ATR-MIR), which involves an internal reflectance of light inside a crystal off the surface in contact with the sample, was also officially validated and adopted by the AOCS and the AOAC.[17,18] Although it was applied to milk fat, preliminary results were unsatisfactory due to the low TFA levels and the heterogeneity of FA with *trans* double bond(s). Moreover, *cis*-, *trans*-, and *trans*,*trans*-CLA absorption bands in the vicinity of 948, 985, and 990 cm^{-1} interfere with isolated MIR measurements, which could be problematic for countries that have excluded *trans*-CLA from the legal definition of TFAs.[19] The latter disadvantage might be overcome by employing another vibrational spectroscopy technique, such as Raman scattering measurement.

Raman spectroscopy is a physical technique based on inelastic scattering of light photons upon interaction with a sample. The energy of the re-emitted photons is shifted up or down in comparison with original laser frequency, which is called the Raman scattering. Contrary to absorption in FT-IR spectroscopy, the *trans*-FA scattering band in Raman spectroscopy is not buried in the fingerprint region of the MIR spectrum but has an isolated specific scattering feature between 1680 and 1640 cm^{-1}.[20] The latter is an advantage, which could be used for more specific determination of individual unsaturated FAs. Already, Meurens et al.[20] successfully employed Fourier transform Raman spectroscopy in determination of total CLA in milk fat. This report continues investigations on individual and total CLA and reports new determinations of individual and total *trans*-MUFA using Raman spectra of bovine milk fat.

MATERIALS AND METHODS

Sample Selection. The sample storage and sample selection methodology were previously described.[21] Briefly, a total of 100 milk

samples were selected from a sample bank (n = 1033) of six different cow feeding experiments aiming at changing the FA profile of dairy products. The sample subset was selected using a genetic algorithm applied to cover the naturally occurring range of several milk FAs of interest (different odd and branched chain saturated FAs and different *trans*-C18:1 and *cis*/*trans*-C18:2 unsaturated isomers) in high, mid, and low concentration ranges.[22] The milk fat was extracted using a previously described methodology involving dichloromethane-ethanol.[23]

FA Standards. Two monounsaturated *trans*-9 and *trans*-10 C18:1 fatty acid methyl ester standards (FAMES) and one *trans*-9 triacylglyceride (TAG) trielaidin standard were purchased from Larodan (Larodan Fine Chemicals, Malmo, Sweden) and Nu-Check (Nu-Check Prep, Inc., MN).

GC Reference Data. Quantification of TFAs and FA groups using spectral data requires precise gas liquid chromatography (GC) reference data for the construction of mathematical models. Identification and quantification of TFA through GC have been greatly improved with new highly polar, long capillary columns, but direct GC without prior fractionation could show overlapping between different *trans-n* and *cis-n* C18:1 positional isomers and *trans-n* C16:1 coelution with specific branched chain saturated and *cis-n* C16:1 monounsaturated FAs, which might result in an underestimation of the total TFA content.[19,21] Here, we used the temperature dependency of the polarity of cyanopropyl phases[24] to mathematically deduce concentrations of overlapping FAs using two different temperature programs without prior fractionation. A similar approach was described before.[21,25,26] After extraction, all samples were methylated,[23] and FAMEs were analyzed by GC according to Vlaeminck et al.[27] (first temperature program) and by an isothermal (T = 180 °C) (second) temperature program. Implementation of both temperature programs without prior separation on silver ion thin-layer chromatography (Ag^+ TLC) allowed quantification of individual *trans*-MUFA, which coelute with branched chain saturated and specific *cis-n* monounsaturated FAs when only one GC temperature program is used. Because of a different separation with the second temperature program, most FA could be quantified individually as previously described.[21,25] As coelution of FA also depends on the column status, the identity of the FA and coeluting peaks regularly requires confirmation by injections of Ag^+ TLC fractions. Because of a limited sample quantity for eight of the 100 selected samples, GC profile reference data were available for 92 milk fat samples only.

Fourier Transform Raman Analysis. All FT-Raman spectra were acquired on a Vertex 70-RAM II Bruker Fourier transform Raman spectrometer (Bruker Analytical, Madison, WI). The instrument is equipped with a Nd:YAG laser (yttrium aluminum garnet crystal doped with triply ionised neodymium) with an output at 1064 nm (9398.5 cm^{-1}). The maximum of the laser power is 1.5 W. The measurement accessory is prealigned, and only the Z-axis of the backscattered light was adjusted to set the sample in the appropriate position regarding the local point and to maximize the scattering intensity. The 180° backscattering refractive geometry, CaF_2 beam splitter, and liquid nitrogen-cooled Ge diode array detector have been used. The OPUS 6.5 software for Windows of Bruker Instruments was used for the instrument management, spectral acquisition, and file transformation. The spectral data were obtained with a resolution of 4 cm^{-1} and a nominal laser power of 600 mW. Milk fat samples and pure FA standards (~0.1−0.5 g/sample) were analyzed in vials selected by CRA-W in previous Fourier transform Raman analysis[28] with PE caps (Klaus Ziemer GmbH, Mannheim, Germany), at room temperature (~25 °C) (RT) and immediately after placing in a freezer at −80 °C for a period of 15 min (FT). To ensure homogenization of the milk fat, all samples were melted at 38 °C in a water bath, at a minimum of 1 h prior to temperature treatment. For each spectrum, 64 scans were coadded and averaged to obtain a good signal-to-noise ratio. A total of 3734 data points were recorded from 0 to 3599 cm^{-1}. Because of very low milk fat

Table 1. FAMES' Vibrational Bands and Intensities As Obtained from Fourier Transform Raman Spectra (Bruker RAM II) at FT (−80 °C) after MSC[a]

trans-9 C18:1		*trans*-11 C18:1		trielaidin TAG	
ν (cm^{-1})	intensity[b]	ν (cm^{-1})	intensity[b]	ν (cm^{-1})	intensity[b]
3020 s	7	3020	7		
3000 s	8	3000 s	11	3000 s	12
2983	5	2985	6	2975 sh	10
2965 s, sh	20	2965 sh	17	2956 sh	19
2952	22	2952	21	2936 sh	33
2933 sh	29	2934 sh	29	2915 sh	32
2916 sh	29	2924 sh	28	2884 s	100
2899 sh	42	2896 b, sh	44	2872 sh	49
2884 s	100	2884 s	100	2860	49
2850	56	2847	50	2847	52
2836 sh	35	2836 sh	30	2757	3
2747 b	3	2745 b	4	2726 b	7
2724 b	7	2724 b	7	2713 sh	5
2709 b, sh	5	2705 b, sh	5	2693 sh	3
2659	2	2659	3	2664	2
1743	5	1743	5	2185	1
1673 s	16	1673 s	12	1743	5
1493 b	1	1487 sh	3	1728	3
1478 sh	3			1672 s	16
1464 s, sh	9	1460 b, sh	10	1493 sh	2
1452	9	1452	10	1464 sh	15
1441 s	19	1441 s	23	1441 s	27
1418 s, sh	13	1418 s, sh	12	1418	3
1333	2	1333	2	1370	3
1314 sh	3	1312 sh	4	1312	5
1298 s	13	1298 s	9	1298 s	20
1284 sh	4	1285	10		
1264 s	3			1264 s	4
1254	2			1254	3
1162	2	1162	2	1227	2
1122 s	6	1115 sh	4	1186	2
1098 s	11	1105 s	13	1162	2
1063 s	9	1063 s	10	1123 s	8
1051 s, sh	3	1030	2	1098 s	10
1041	2	1017	2	1062 s	12
1004 b	1	997	3	1051 sh	4
891 sh	5			1041	3
886 s	6	887 s	6	899 sh	3
557	1	556	2	891 s	5
496	2	496	2	776	2
400	2	390	3	606	2
331	3	331	3	557	2
231	3	253 b	3	547	2
192 b	4	245 b, sh	3	360	2
170	5	167 b, sh	4	266	3
146 sh	3	149	6	248	2
125 s	6	114 b, sh	5	215 b	7
102 sh	7	99 b, sh	9	168 b	6
84 s	13	75 s	15	84 b	18

[a] The letter "b" indicates a broad vibrational band, the letter "s" indicates a sharp vibrational band, and the letters "sh" indicate a shoulder band. [b] Intensity in % of maximum peak in the vicinity of 2884 cm^{-1}.

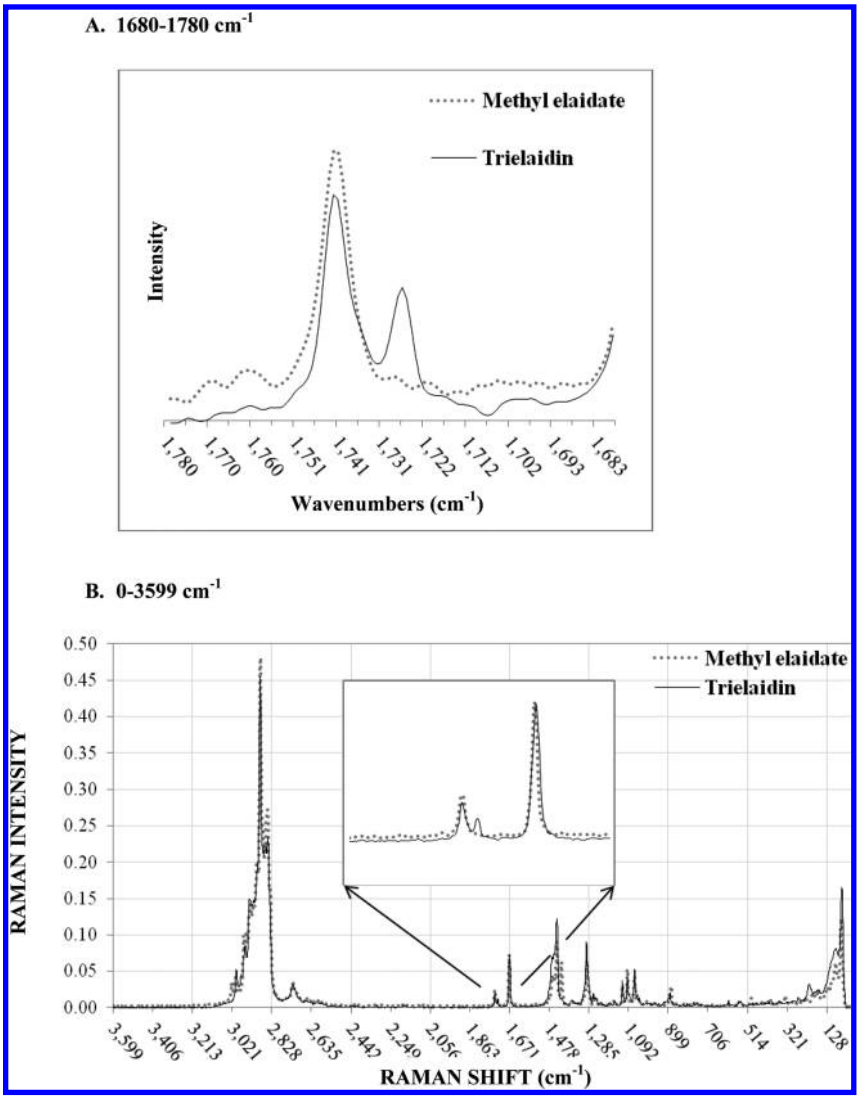

Figure 2. MSC Raman spectra of solid (after freezing at −80 °C) *trans*-9 C18:1 FAME (elaidate, dotted) vs solid *trans*-9 C18:1 TAG (trielaidin, full) in the (A) 1780−1680 and (B) 0−3599 cm^{-1} scattering regions [*x*-axis, wavenumbers (cm^{-1}); *y*-axis, scattering intensity].

quantity in 14 and extraction solvent contamination in three of all 92 selected samples, Fourier transform Raman spectroscopy data in RT and FT were available for 75 milk fat samples.

Data Treatment. Data incorporation, pretreatment, and modeling were performed as previously described.[21] The OPUS spectra files were converted to the jcamp-dx file system, which was imported into The Unscrambler v.7.1 software (CAMO, Trondheim, Norway). The preprocessing method of choice was multiplicative scatter correction (MSC), which compensates for undesired variation in the scattering intensity caused by various multiplicative effects and laser power fluctuations. Standard partial least-squares (PLS) regression was carried out in combination with the uncertainty testing "jackknife" procedure in The Unscrambler program, which is used to select variables that correlated with the measured parameter and to reject data from Raman shifts not contributing to the prediction. For all PLS models, validation was carried out using systematic cross-validation with three folds and 25 units per segment. The optimal number of PLS factors used for the regression was determined from the minimum residual validation variance.

PLS regression was performed according to two different strategies, which differed in the number of predictor variables used (selected spectral regions vs full spectral range). For the selected spectral regions, Raman spectra were reduced from 3734 to 1650 variables, by including only regions that are commonly believed to be the carriers of the chemical information (3100−2600 and 1850−750 cm^{-1}).[28] PLS|A consisted of using PLS regression with selected scattering regions (1650 variables), and PLS|B consisted of using PLS with the full Raman spectra (3734 variables). In addition, each of the PLS|A and PLS|B methods were performed for RT only, FT only, and concatenated RT and FT spectra (RFT). A total of six prediction models for each of the individual *trans*-MUFAs (*trans*-4 C18:1, *trans*-5 C18:1, *trans*-6 + 7 + 8 C18:1, *trans*-9 C18:1, *trans*-10 C18:1, *trans*-11 C18:1, *trans*-12 C18:1, and *trans*-15 C18:1) and both *trans*-MUFA and CLA FA groups were built when using the Raman spectra of all 75 milk samples (Table 3). Furthermore, to better evaluate the prediction performance for minor FAs in their most common concentration range (below 1% total fat) and to avoid overfitting based on discontinuous data set distribution, milk fat samples with high amounts of specific individual FAs (such as *trans*-10 C18:1, *trans*-11 C18:1, and *trans*-12 C18:1) were removed, and new PLS models were constructed using only the remainder (Table 3). No other criteria or software tools were used to eliminate any additional samples.

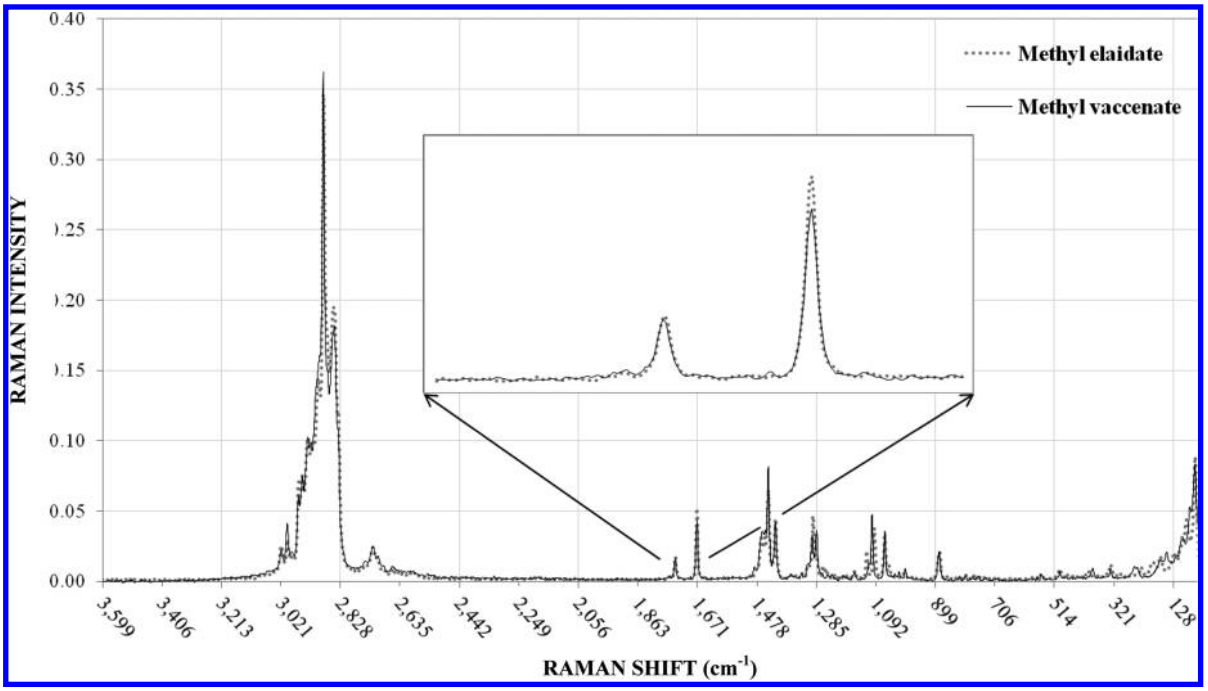

Figure 3. MSC Raman spectra of solid (after freezing at −80 °C) *trans*-9 C18:1 FAME (elaidate, dotted) vs solid *trans*-11 C18:1 FAME (vaccenate, full) in the 0−3599 cm^{-1} scattering region [*x*-axis, wavenumbers (cm^{-1}); *y*-axis, scattering intensity].

RESULTS

Spectral Observations. Full multiplicative scatter corrected (MSC) Raman spectra derived at RT and immediately after freezing at −80 °C (FT) of pure *trans*-9 C18:1 (elaidate) and *trans*-11 C18:1 (vaccenate), FAMES can be found in Figure 1A, B, respectively. A detailed description of the Raman shifts and corresponding Raman intensities from spectra of pure elaidate and vaccenate FAMES derived in FT conditions can be found in Table 1. In general, FT-derived spectra of FAMES revealed many additional well-defined Raman scattering bands in the vicinity of 3020, 2965, 2952, 1418, 886, 557, 331, 231, 192, 170, 125, 102, and 84 cm^{-1} (elaidate) and 3020, 2965, 2952, 1418, 887, 556, 331, 253, 167, 114, 149, 99, and 75 cm^{-1} (vaccenate), when compared to the Raman spectra at RT.

While the FT spectra of elaidate and vaccenate showed an increase in Raman scattering intensity in the vicinity of 2890 (shifted to 2884 cm^{-1}), 2724, 1743, 1669 (shifted to 1673 cm^{-1}), 1441, 1301 (shifted to 1298 cm^{-1}), 1122, and 1098 cm^{-1}, which was similar to spectral perturbations tendency previously demonstrated with the FT spectra of milk fat,[21] some of the scattering features in the lower wavenumbers (such as 886, 557, 496, 331, and 231 cm^{-1}) had not been previously observed with saturated FAMES or milk fat samples.

Whether the spectral dynamics of TAGs, which are the dominant lipid component in milk fat, follow these new Raman scattering features shown with FAMES was demonstrated by the analysis of *trans*-9 C18:1 TAG (trielaidin) in both RT and FT. As compared to the methyl esters, the carboxylic group in TAG is connected to a glycerol backbone, which causes an additional Raman vibrational mode of the C═O bond in the vicinity of 1728 cm^{-1} (Figure 2A) when analyzed at FT.

Nevertheless, the spectra of elaidate and trielaidin looked analogous, and most of the important features (with an exception of sharp vibrational intensity at 3020 cm^{-1} and two weak scattering peaks in the vicinity of 496 and 331 cm^{-1} present in the methyl ester, but not in the TAG), such as the C═C stretching vibration scattering near 1673 cm^{-1}, the methylic groups vibration in the vicinity of 2884 cm^{-1}, and the stretching vibration of the ethylenic C−H bonds near 3000 cm^{-1}, were similar in wavenumber position and scattering intensity for both elaidate and trielaidin (Figure 2B and Table 1). Furthermore, features in the very low wavenumber region (200−50 cm^{-1}) between the FAMES and the TAG Raman spectra, which might be associated with crystallization dynamics of the FA backbone, are somewhat different in scattering intensity and position.

The latter suggests that monounsaturated FAMES could be a sufficient alternative for Raman investigations of most molecular

Table 2. Concentration Range of Individual and Grouped *trans*-MUFA and CLA FAs in Milk Fat (g/100 g of FAME, *n* = 75)

FA	min	max	avergae	SD
trans-4 C18:1	0.006	0.074	0.020	0.010
trans-5 C18:1	0.006	0.108	0.018	0.015
trans-6 + 7 + 8 C18:1	0.105	1.079	0.254	0.157
trans-9 C18:1	0.113	1.155	0.232	0.181
trans-10 C18:1	0.113	11.74	0.945	2.320
trans-11 C18:1	0.170	4.925	0.950	0.908
trans-12 C18:1	0.125	1.424	0.316	0.220
trans-15 C18:1	0.023	0.515	0.152	0.103
trans-MUFA[a]	1.475	21.01	4.538	4.168
cis-9,*trans*-11 C18:2	0.005	1.958	0.437	0.405
trans-10,*cis*-12 C18:2	0.000	0.038	0.013	0.008
CLA[b]	0.056	2.041	0.472	0.446

[a] Individual FAs reported as well as all-*trans* C14:1 and all-*trans* C16:1 are included in the sum of *trans*-MUFA. [b] Individual FAs reported as well as *trans*-9,*cis*-11 C18:2 and *trans*-11,*cis*-13 + *cis*-9,*cis*-11 C18:2 are included in the sum of CLAs.

Table 3. Partial Least Squares Regression Results for Individual and Grouped *trans*-MUFA and CLA FAs Using Selected Windows (750−1800 and 2750−3100 cm^{-1}, PLSA) and Full Region (0−3599 cm^{-1}, PLSB) for Raman Spectra of Milk Fat Samples Analyzed at RT, after Solidification at −80 °C (FT) and a Combination of RMF and FMF (RFT) Spectra (n = 75)[a]

		RT		FT		RFT	
		PLSA	PLSB	PLSA	PLSB	PLSA	PLSB
trans-4 C18:1	R^2	0.159	0.190	0.323	**0.633**	0.165	0.466
n = 75	RMSECV[b]	0.010	0.009	0.008	**0.006**	0.010	0.008
max[c]	no. PLS	2	2	4	4	1	6
trans-5 C18:1	R^2	0.536	0.507	0.600	0.502	**0.612**	0.592
n = 75	RMSECV	0.010	0.011	0.010	0.011	**0.009**	0.010
max[c]	no. PLS	4	3	4	3	**5**	7
trans-6/7/8 C18:1	R^2	0.577	0.553	0.565	0.816	0.595	**0.880**
n = 73	RMSECV	0.052	0.054	0.053	0.035	0.051	**0.028**
<0.50 g/100 g FAME	no. PLS	3	3	2	4	3	**6**
trans-6/7/8 C18:1	R^2	0.351	0.338	0.396	0.350	0.238	0.257
n = 75	RMSECV	0.127	0.129	0.122	0.127	0.139	0.138
max[c]	no. PLS	10	10	4	3	3	4
trans-9 C18:1	R^2	0.798	0.812	0.714	0.861	0.826	**0.901**
n = 70	RMSECV	0.029	0.028	0.035	0.025	0.027	**0.020**
<0.42 g/100 g FAME	no. PLS	4	3	4	4	4	**5**
trans-9 C18:1	R^2	0.859	0.851	**0.874**	0.867	0.857	0.864
n = 75	RMSECV	0.055	0.056	**0.052**	0.053	0.055	0.054
max[c]	no. PLS	3	3	**5**	5	2	3
trans-10 C18:1	R^2	0.361	0.340	0.622	**0.756**	0.735	0.389
n = 68	RMSECV	0.122	0.125	0.097	**0.076**	0.079	0.120
<0.84 g/100 g FAME	no. PLS	1	4	4	**4**	0	3
trans-10 C18:1	R^2	0.933	0.933	0.906	0.911	**0.939**	0.944
n = 75	RMSECV	0.606	0.605	0.710	0.686	**0.573**	0.564
max[c]	no. PLS	6	6	4	6	**7**	9
trans-11 C18:1	R^2	**0.686**	0.372	0.622	0.659	0.639	0.537
n = 66	RMSECV	**0.120**	0.173	0.133	0.130	0.129	0.148
<1.2 g/100 g FAME	no. PLS	**7**	5	4	5	5	7
trans-11 C18:1	R^2	**0.914**	0.923	0.882	0.860	0.910	0.887
n = 75	RMSECV	**0.264**	0.250	0.307	0.335	0.269	0.301
max[c]	no. PLS	**6**	8	4	4	4	4
trans-12 C18:1	R^2	0.779	0.783	**0.843**	0.773	0.782	0.763
n = 73	RMSECV	0.072	0.071	**0.061**	0.073	0.071	0.074
<0.91 g/100 g FAME	no. PLS	6	5	**4**	3	2	3
trans-12 C18:1	R^2	0.771	0.790	0.769	0.765	**0.789**	0.770
n = 75	RMSECV	0.105	0.101	0.105	0.106	**0.101**	0.105
max[c]	no. PLS	7	8	4	3	**2**	3
trans-15 C18:1	R^2	0.227	0.514	0.426	**0.701**	0.575	0.668
n = 75	RMSECV	0.090	0.075	0.079	**0.056**	0.069	0.060
max[c]	no. PLS	2	7	4	**6**	7	7
trans-MUFA	R^2	0.763	0.809	0.678	**0.866**	0.859	0.626
n = 63	RMSECV	0.306	0.272	0.353	**0.228**	0.237	0.381
<4.6 g/100 g FAME	no. PLS	7	4	2	**5**	6	3
trans-MUFA	R^2	0.933	0.928	0.835	0.878	0.943	**0.944**
n = 70	RMSECV	0.280	0.292	0.440	0.381	0.260	**0.255**
<8.1 g/100 g FAME	no. PLS	7	7	4	5	9	**6**
trans-MUFA	R^2	**0.987**	0.981	0.937	0.943	0.981	0.977
n = 75	RMSECV	**0.472**	0.575	1.038	0.992	0.591	0.634
max[c]	no. PLS	**7**	8	3	3	8	5
cis-9, *trans*-11 C18:2	R^2	0.851	0.853	0.833	0.851	**0.859**	0.835
n = 75	RMSECV	0.167	0.166	0.177	0.167	**0.162**	0.176

Table 3. Continued

		RT		FT		RFT	
		PLSA	PLSB	PLSA	PLSB	PLSA	PLSB
max[c]	no. PLS	6	6	5	4	**7**	4
trans-10, *cis*-12 C18:2	R^2	0.290	0.258	0.362	**0.844**	0.662	0.823
n = 75	RMSECV	0.007	0.007	0.007	**0.003**	0.005	0.003
max[c]	no. PLS	2	5	3	**6**	7	9
CLA	R^2	0.852	**0.948**	0.918	0.909	0.945	0.895
n = 75	RMSECV	0.171	**0.101**	0.127	0.133	0.104	0.144
max[c]	no. PLS	3	**7**	4	5	6	6

[a] Best results (highlighted) are based on lowest RMSECV and $R^2 > 0.50$. [b] Root mean square error of cross-validation in g/100 g FAMEs. [c] Indicates the maximum concentration in g/100 g FAME of the corresponding FA or FA group as reported in Table 2.

Table 4. Intercept, Slope, and Bias Regression Parameters of Selected Models for Prediction of Individual and Grouped *trans*-MUFA and CLA FAs Using Selected Windows (750−1800 and 2750−3100 cm^{-1}, PLSA) and Full Region (0−3599 cm^{-1}, PLSB) for Raman Spectra of Milk Fat Samples Analyzed at RT, after Solidification at −80 °C (FT), and a Combination of RT and FT (RFT) Spectra (n = 75)

FA	*trans*-4 C18:1	*trans*-5 C18:1	*trans*-6/7/8 C18:1	*trans*-9 C18:1[a]	*trans*-9 C18:1	*trans*-10 C18:1[a]	*trans*-10 C18:1	*trans*-11 C18:1[a]	*trans*-11 C18:1
model	FT PLSB	RFT PLSA	RFT PLSB	RFT PLSB	FT PLSA	FT PLSB	RFT PLSA	RT PLSA	RT PLSA
intercept	0.007	0.006	0.022	0.019	0.027	0.064	0.031	0.189	0.107
slope	0.634	0.782	0.899	0.896	0.884	0.815	0.969	0.727	0.884
BIAS	0.000	0.001	0.002	0.001	0.002	0.001	0.004	0.006	0.005

FA	*trans*-12 C18:1[a]	*trans*-12 C18:1	*trans*-15 C18:1	*trans*-MUFA[b1]	*trans*-MUFA[b2]	*trans*-MUFA	*cis*-9, *trans*-11 C18:2	*trans*-10, *cis*-12 C18:2	CLA
model	FT PLSA	RFT PLSA	FT PLSB	FT PLSB	RFT PLSB	RT PLSA	RFT PLSA	FT PLSB	RT PLSB
intercept	0.033	0.072	0.032	0.405	0.169	0.129	0.052	0.001	0.018
slope	0.887	0.764	0.837	0.930	0.951	0.973	0.881	0.889	0.952
BIAS	0.000	0.003	0.006	0.002	0.005	0.005	0.003	0.003	0.005

[a] Indicates the best PLS model for an individual FA in minor concentration (lower than 1.0 g/100 g FAME) as indicated in Table 3. [b] Indicates the best PLS model for *trans*-MUFA in concentration with a maximum of 1, 4.6 g/100 g (n = 63); and 2, 8.1 g/100 g (n = 70) FAME.

structure features in different FAs but might not be a suitable option for interpretation of spectral perturbations due to crystallization dynamics at freezing temperatures in the lower wavenumber regions of the Raman spectrum.

Raman scattering caused by the difference in position of the *trans* C═C bond in the FA chain between elaidate and vaccenate was investigated. The vibrational feature of the elaidate in the vicinity of 1673 cm^{-1} showed an increase in scattering intensity (∼ 12%) as compared to the vaccenate, but no frequency shifts due to the *trans* C═C bond location in the FA backbone were evident (Figure 3). The latter could complicate differentiation of the two FAs in quantification models with milk fat spectra.

Milk FA Composition. An overview of the results from the reference GC analyses is presented in Table 2. Because of an influence from the diet, the total *trans*-MUFAs were present in very high concentrations and ranged from 1.5 to 21 g/100 g. Total CLAs maximally represented 2.0 g/100 g of milk fat (Table 2). Furthermore, insufficient GC resolution prevented reliable separation of individual *trans*-6 C18:1, *trans*-7 C18:1, and *trans*-8 C18:1 FA isomers but allowed accurate determination of the *trans*-6 + 7 + 8 C18:1 sum. The reference data cross-correlation results between the individual FAs and the major FA groups indicated a high correlation ($R^2 > 0.95$) between *trans*-10 and *trans*-11 C18:1 and *trans*-MUFA and between *cis*-9,*trans*-11 C18:2 and CLA total group, as well as a low cross-correlation ($R^2 < 0.30$) between the *trans*-10,*cis*-12 C18:2 isomer and the CLA or *trans*-MUFA total groups.

PLS Results. PLS regression with cross-validation was performed on selected spectral bands (PLS|A) and full range Raman spectra (PLS|B) using all milk fat samples (n = 75) analyzed at two different temperature conditions: at RT (∼25 °C) and immediately after freezing the milk fat at −80 °C (FT). The validation coefficient of determination (R^2), the root-mean-square error of cross-validation (RMSECV, g/100 g FAME), and the number of PLS factors for *trans*-MUFA and CLA groups, as well as for the individual *trans*-MUFA, are presented in Table 3. Intercept, slope, and bias parameters of the best prediction models are presented in Table 4.

In general, the total CLA group and the two major *cis*-9,*trans*-11 C18:2 and *trans*-10,*cis*-12 C18:2 CLA isomers were predicted successfully, with coefficients of determination (R^2) of 0.95, 0.86, and 0.84 and RMSECV equal to 0.101, 0.162, and 0.003, respectively (Table 3). The PLS regression coefficients plot for the best (FT with PLS|B) *trans*-10,*cis*-12 C18:2 model indicated four main wavenumbers (1653, 1451, 2849, and 1666 cm^{-1}) and

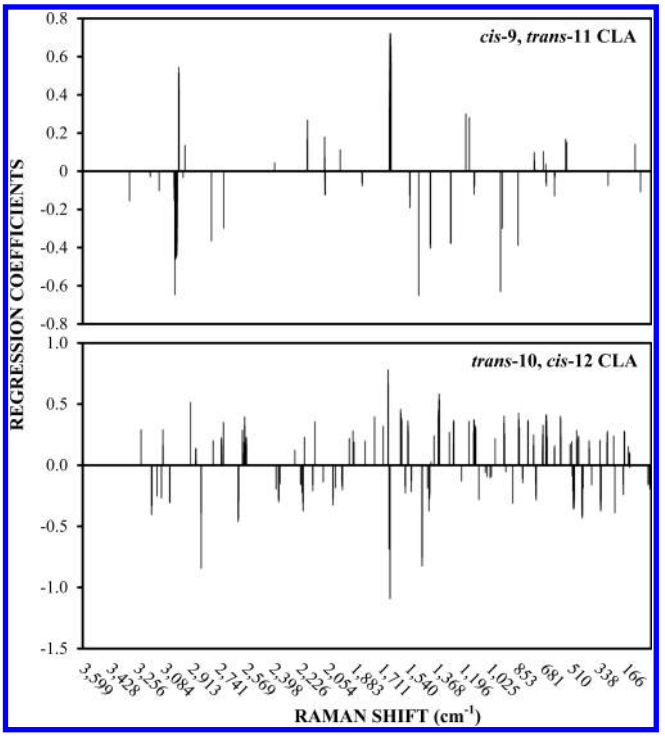

Figure 4. PLS regression coefficients for prediction of the *cis*-9,*trans*-11 and *trans*-10,*cis*-12 CLAs using Raman spectra of solid (after freezing at −80 °C, FT) milk fat in the 0−3599 cm^{-1} scattering region [*x*-axis, wavenumbers (cm^{-1}); *y*-axis, regression coefficients value].

numerous other less contributing wavenumbers in the lower region of the Raman spectrum (Figure 4). The most important regression coefficients for the *cis*-9,*trans*-11 C18:2 models were similar to the regression coefficients of the CLA group and appeared in the vicinity of 1656−1646 cm^{-1}. These regression coefficients coincide with previously reported scattering peaks of pure FAMES.[20] However, the uncertainty "jackknifing" test did not select 1438 cm^{-1} as an important information carrier for *cis*-9, *trans*-11 C18:2, and other regression coefficients near 3017, 3015, 3002, 2990, and 1472 cm^{-1} appeared as major contributors (Figure 4).

Predictions for *trans*-10 C18:1 (R^2 = 0.94) and *trans*-11 C18:1 (R^2 = 0.91), as well as for the *trans*-MUFA group (R^2 = 0.99) had the best model parameters when compared to all other individual and group FA models (Table 3). The latter was a consequence of some samples with very high concentrations of the two FAs, which influenced predictions for the total *trans*-MUFA group (Figure 5). Furthermore, samples with a high content of these major FAs were removed, and models were evaluated based on minor (below 1.0 g/100 g FAME) concentrations for *trans*-10 C18:1 and *trans*-11 C18:1 (Figure 5), as well as low (below 5.0 g/100 g FAME) concentrations for the *trans*-MUFA group (Table 3). Model performance for *trans*-10 C18:1 and *trans*-11 C18:1 diminished (R^2 = 0.76 and R^2 = 0.69 with RMSECV of 0.076 and 0.120, respectively), while the prediction of the *trans*-MUFA group remained very well (R^2 = 0.87, RMSECV = 0.228 with five PLS components). The regression coefficients plot in The Unscrambler indicated that the best *trans*-10, *trans*-11, and all-*trans*-MUFA group prediction models were largely determined by important variables in the 1664−1674 cm^{-1} wavenumber range (Figure 6).

No deterioration in prediction performance was apparent with the best PLS model of *trans*-9 C18:1 in very low concentration (0.42 g/100 g, R^2 = 0.90) as compared to the model using the maximum concentration (1.2 g/100 g, R^2 = 0.87) and the full data set of 75 samples (Table 3). Similar performance was evident for the *trans*-12 C18:1 isomer, which resulted in R^2 = 0.79 for the full model and R^2 = 0.84 for the low concentration model with maximum amounts of 1.4 g/100 g and 0.91 g/100 g in milk fat, respectively (Table 3).

Furthermore, the *trans*-6 + 7 + 8 C18:1 sum was not predicted well when using all 75 samples. Upon removal of two milk fat samples with the highest concentrations of *trans*-6 + 7 + 8 C18:1, the concentration maximum decreased to 0.50 g/100 g FAME, and the cross-correlation with the *trans*-MUFA group diminished from R^2 = 0.52 (n = 75) to R^2 = 0.42 (n = 73). Nevertheless, an immediate improvement in all-*trans*-6 + 7 + 8 C18:1 models was apparent, with PLS|B having the best model parameters (R^2 = 0.88, RMSECV = 0.028 and six PLS components) and very different regression coefficients. In addition to 1673 cm^{-1}, which was the main important variable in the full data set models, the low concentration *trans*-6 + 7 + 8 C18:1 models were influenced by several other significant variables in the vicinity of 1652, 1687, 3040, 3030, 2960, 2820, 257, 330, and 435 cm^{-1} (listed in order of decreasing regression coefficient).

To evaluate specificity for the scattering signal from individual FAs, the total abundance ratio of the reference data for individual *trans*-FA in the *trans*-MUFA group was calculated and then predicted using PLS regression. Predictions of these ratios indicated a high (R^2 = 0.89) and moderate (R^2 = 0.64) specificity for *trans*-6 + 7 + 8 C18:1/*trans*-MUFA and *trans*-9 C18:1/*trans*-MUFA, respectively. The *trans*-10/*trans*MUFA and *trans*-11/*trans*-MUFA total abundance ratios showed no specificity (R^2 < 0.40).

In addition, the sums of specific FAs with similar molecular structure features were modeled. The PLS results indicated that the sum of *trans*-4 + 5 C18:1 was predicted better (R^2 = 0.67) as compared to either *trans*-4 only or *trans*-5 only and the sum of *trans*-11 + 12 C18:1 in low concentrations (maximum of 1.5 g/100 g FAME, n = 66) was drastically improved (R^2 = 0.85) as compared to the predictions of either the *trans*-11 or the *trans*-12 only FAs in minor concentrations. GC data cross-correlation between the sums and the total *trans*-MUFA group did not increase as compared to the cross-correlations of the individual FAs.

DISCUSSION

FA Standards. Raman spectra of saturated FAMES and milk fat samples analyzed after freezing at −80 °C (FT) have recently been shown to exhibit increased scattering in different C−H vibrational frequencies as compared to liquefied or RT spectra.[21] Here, *trans* monounsaturated standards seemed to exhibit a different level of crystallization as more bands with sharper, narrower, and larger Raman scattering intensity, related to C−H and possibly C−C−C− vibrations, were observed. Differences in the −80 °C versus RT analyzed Raman spectra of elaidate and vaccenate indicated a considerably higher amount of new and sharper scattering features as compared to previously analyzed odd and branched chain saturated FAMES.[21] The latter might be a result of the *trans* C=C bond presence in the FAs chain, which further influences the melting temperature (higher mp of *trans*-FA vs branched saturated FA) and crystallization dynamics of *trans*-FAMES molecules in freezing conditions as compared to saturated FAMES.[21] Furthermore, few perturbations in the *trans*

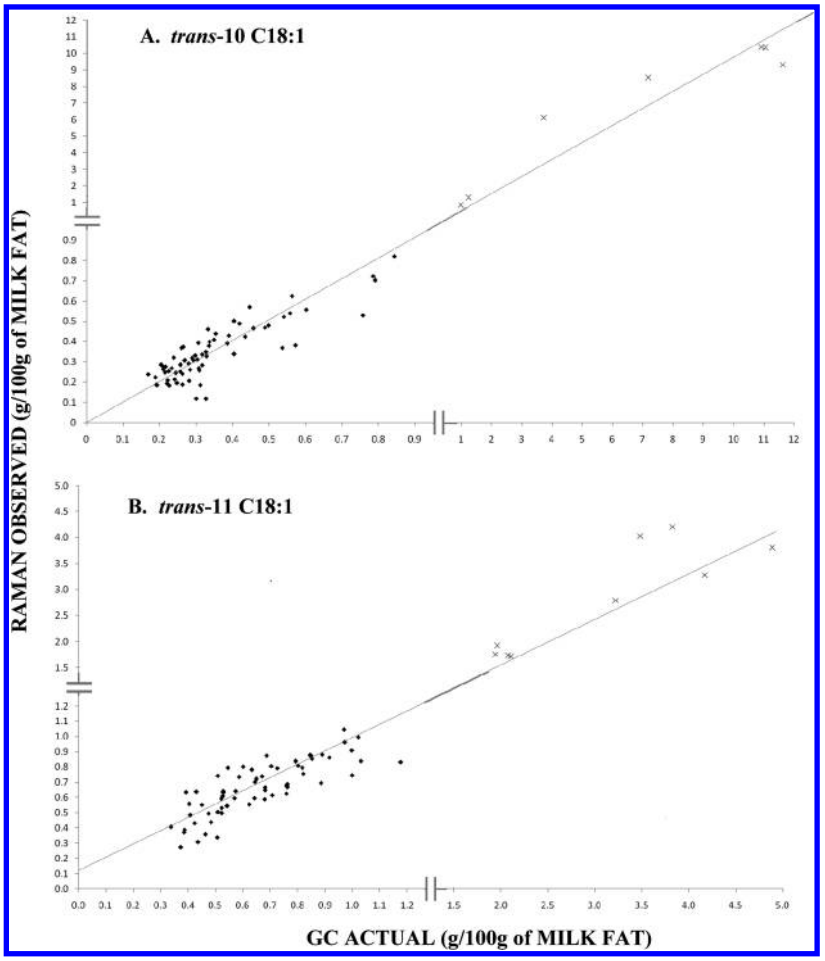

Figure 5. Validation PLS plots of the most robust prediction models for (A) *trans*-10 C18:1 and (B) *trans*-11 C18:1 FAs (as indicated in Tables 3 and 4) using samples with minor concentrations only (full square symbols) and before removal of samples with very high concentrations (X symbols) of the two FAs in g/100 g FAME.

C═C unsaturation region were evident. The spectra of pure *trans*-monounsaturated FAMES and the trielaidin TAG indicated an upfield shift of the *trans* C═C peak from 1669 cm^{-1} in RT to 1673 cm^{-1} in FT. Also, a similar shift (~4 cm^{-1}) was observed with *cis* monounsaturated FAMES; thus, the additive spectral dynamics (combined shift) of the 1620−1690 cm^{-1} region are not likely to drastically affect prediction models using spectra obtained at both temperature conditions (Figure 7). Nevertheless, there might be a minor separation between the *trans* and the *cis* C═C related signals in FT due to changes in the scattering intensity and differences in line shape profile as compared to RT (Figure 7). Moreover, the Raman spectra of milk fat at FT did not show any significant wavenumber shifts in the 1620−1690 cm^{-1} scattering region as compared to RT, although some minor perturbations of the line shape in some of the milk fat spectra were evident.[21]

RT versus FT PLS Predictions. The prediction abilities of RT, immediately after freezing at −80 °C (FT) and concatenated RT and FT (RFT) Raman spectra of milk fat, for the quantification of individual and grouped *trans*-MUFA and CLA FAs, were compared. Because a major part of the scattering information specific to TFAs is contained in the 1660−1690 cm^{-1} C═C stretching vibration, which did not show any drastic milk fat spectral perturbations between FT or RT, most major and minor FAs and the FA groups were equally predicted with Raman spectra analyzed at RT or FT. For example, *cis*-9, *trans*-11 CLA, total CLA, individual *trans*-9 C18:1, *trans*-10 C18:1, and *trans*-11 C18:1 FAs and the total *trans*-MUFA group were similarly predicted using spectra either at RT or FT. However, some individual FAs in limited concentrations, such as *trans*-4 C18:1, *trans*-10 C18:1, and *trans*-10,*cis*-12 CLA were significantly better predicted with FT spectra only (Table 3). The latter might have been influenced by other regression coefficients emerging as important in the lower wavenumber region (50−750 cm^{-1}) of the Raman spectra (Figures 4 and 6).

PLS models for the *trans* 6 + 7 + 8 C18:1 sum in low concentration (maximum 0.50 g/100 g FAME, n = 73) were also better when FT was used, but all *trans* 6 + 7 + 8 C18:1 models using the full data set of 75 milk fat samples showed a drastically decreased performance (Table 3). This low performance improved significantly after the removal of two samples with the highest concentration of *trans*-6 + 7 + 8 C18:1. Upon investigation of the regression coefficients for the full data set models, it was noticed that PLS relied mainly on the signal from these two samples, which coincidentally had a very high content of *trans*-10 C18:1 and *trans*-11 C18:1. The variable selection algorithm in combination with the PLS regression initiated a selection of variables related to the high *trans*-10 and *trans*-11 concentrations

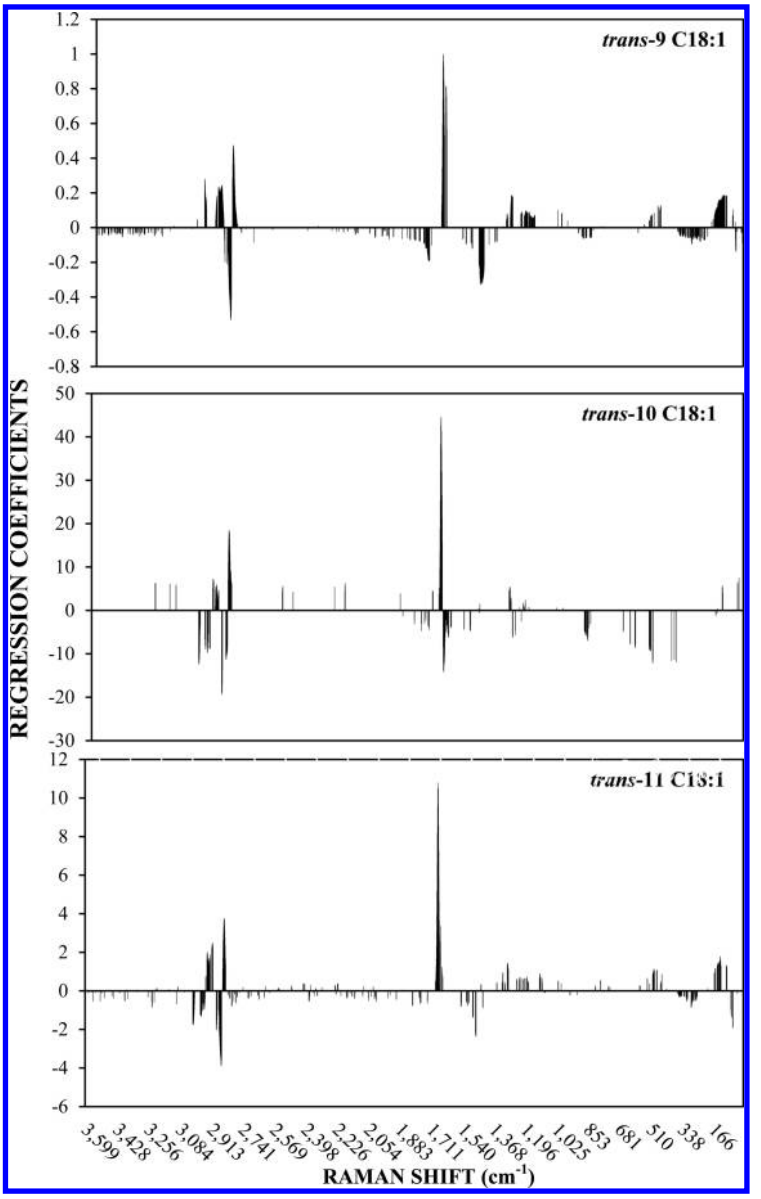

Figure 6. PLS regression coefficients for prediction of *trans*-9,*trans*-11 and *trans*-10 C18:1 FAs using Raman spectra of RT milk fat in the 0−3599 cm^{-1} scattering region [*x*-axis, wavenumbers (cm^{-1}); *y*-axis, regression coefficients value].

(Figure 6), such as in the vicinity of 1674−1664 cm^{-1}, and eliminated other important variables for *trans*-6 + 7 + 8 C18:1, which later emerged in the low concentration data set. Variables in the vicinity of 257, 330, and 435 cm^{-1} had significant regression coefficients and contributed to the *trans* 6 + 7 + 8 C18:1 determination using Raman spectra at FT. The possibility of the *trans*-6 + 7 + 8 C18:1 predictions resulting from of a high cross-correlation with the *trans*-MUFA group was ruled out (*trans* 6 + 7 + 8 C18:1 versus *trans*-MUFA, $R^2 = 0.42$).

Furthermore, it was not possible to associate the reported wavenumbers in the lower region of the Raman spectrum of these minor FAs with known chemical bond vibrations, due to the limited amount of reference data. Analysis and comparison of the Raman spectra from the corresponding pure *trans* TAG isomers could reveal the origin of the reported scattering features, but these minor FAs were not commercially available in the form of TAG or FAMES and should be obtained (purified or chemically synthesized) in significant quantities (>50 mg) in order to be analyzed.

Individual *trans*-MUFA Differentiation. Nevertheless, it might be possible to deduce the extent to which a spectrum contains individual information related to a specific FA without using pure standards, that is, predicting the total abundance ratio [calculated as the ratio of the gas chromatography reference data for that FA over the main group to which it belongs (e.g., *trans*-9 C18:1/*trans*-MUFA) and thus "eliminating" any signal correlation from other FAs with similar molecular structure features]. For example, the good performance and the very different regression coefficients resulting for the low concentration *trans*-6 + 7 + 8 model might indicate a specific signal related to this FA group. Thus, to evaluate the level of *trans*-6 + 7 + 8 C18:1 specificity, the total abundance ratio for this FA sum in the *trans*-MUFA group (*trans*-6 + 7 + 8 C18:1/*trans*-MUFA) was predicted using PLS regression. Results for the *trans*-6 + 7 + 8 C18:1/*trans*-MUFA

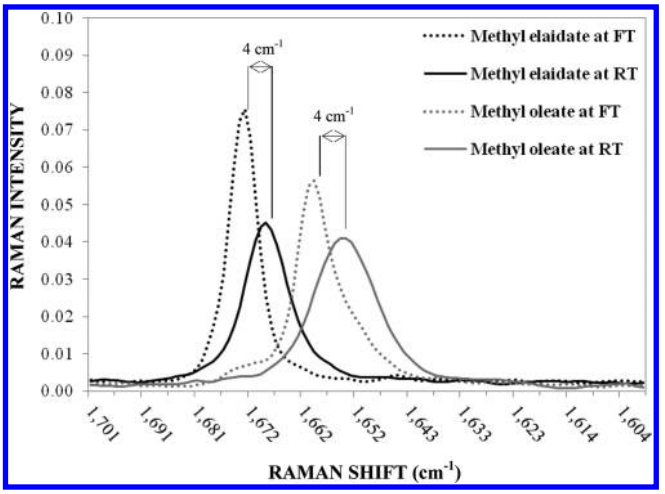

Figure 7. MSC Raman spectra of solid (after freezing at −80 °C, FT, black, dotted) and RT (black, full) *trans*-9 C18:1 (elaidate) FAME vs *cis*-9 C18:1 (oleate) FAME at FT (gray, dotted) and RT (gray, full) in the 1600−1701 cm^{-1} scattering region [*x*-axis, wavenumbers (cm^{-1}); *y*-axis, scattering intensity].

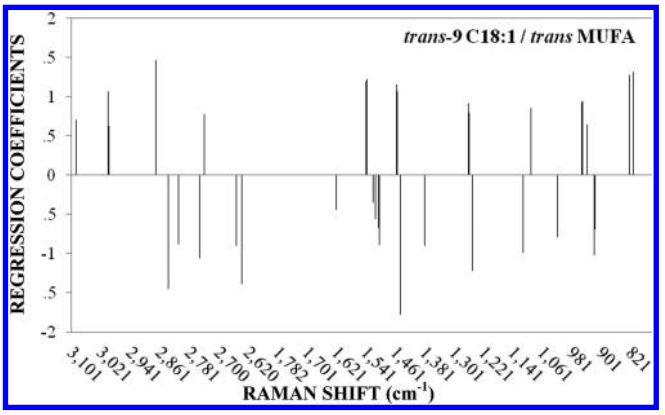

Figure 8. PLS regression coefficients of the *trans*-9 C18:1/*trans*-MUFA ratio using Raman spectra of solid (after freezing at −80 °C, FT) milk fat in the 750−1850 and 2600−3100 cm^{-1} scattering region [*x*-axis, wavenumbers (cm^{-1}); *y*-axis, regression coefficients value].

ratio indicated a high (R^2 = 0.89) specificity. This excellent performance of the abundance ratio model and the unique *trans*-6 + 7 + 8 C18:1 regression coefficients might suggest that the scattering related to the *trans* C═C bond position in the *trans*-6 C18:1, *trans*-7 C18:1, and *trans*-8 FAs is different as compared to *trans*-10 or *trans*-11 C18:1, as well as an additive effect of the combined FAs might be present.

The hypothesis of an additive effect was evaluated by summing low concentration FAs with similar molecular structure features and predicting these sums using PLS regression. The results indicated that the *trans*-4 + 5 C18:1 and the *trans*-11 + 12 C18:1 sums were better determined when compared to the best PLS models for either of the corresponding individual FAs. No increase in the reference data cross-correlation between the FA sums and the *trans*-MUFA group occurred; thus, these improvements must be the result of a scattering signal overlay.

It would seem that FAs grouped by chemical bond location could be predicted better; thus, they might have similar Raman scattering features. Therefore, monounsaturated FAs with different *trans* bond locations could be grouped as near (indicating close vicinity with C═O, such as *trans*-4−8 C18:1), mid (middle of the FA chain, such as *trans*-9−12 C18:1), or far (indicating closeness to the end of the FA chain, such as *trans*-13−16 C18:1), depending on the proximity of the C═C bond to the C═O group. The same rule could also be applied to *cis* monounsaturated FAs. In general, when it comes to chemometrical investigations and predictions of FA constituents in different fat or oil matrices, creating subgroups of FAs based on common structural features could be a way for improvement of quantification models. From a chemometrical point of view, the latter seems a logical approach, but it could be a significant drawback in tasks that require taking decisions on individual FAs with very different physiological roles and yet very similar molecular structure features.

For example, *trans*-11 C18:1 is an important beneficial FA, which is converted to the *cis*-9,*trans*-11 CLA isomer by the action of stearoyl-CoA desaturase in tissue,[29] while the *trans*-10 C18:1 FA is known to have detrimental effects to health and particularly to cardiovascular function via an increase in total TAG concentrations.[30] Thus, differentiation between both FAs when applying different spectrophotometrical quantification models in various dairy food matrices would be of interest. The current data set indicated that while the *trans*-10 and *trans*-11 C18:1 FAs in low concentrations were favorably predicted, this was most probably due to high cross-correlation with the total *trans*-MUFA reference data. Indeed, PLS predictions of the *trans*-10/*trans*MUFA and *trans*-11/*trans*MUFA total abundance ratios showed no specificity. The latter is driven by the *trans* C═C scattering vibrations overlap in both FAs.

The *trans*-9 18:1 FA was predicted very well in both minor and very low concentrations. The better *trans*-9 C18:1 models could be a consequence of the high cross-correlation with the *trans*-10 (*trans*-9 vs *trans*-10, R^2 = 0.67) and *trans*-11 (*trans*-9 vs *trans*-11, R^2 = 0.85) isomers. The most important regression coefficients for the best *trans*-9 C18:1 and *trans*-11 C18:1 prediction models were in the vicinity of 1668−1679 cm^{-1} (Figure 6), which is in support of the FAMES' spectral observations showing no vibration frequency shifts due to positional differences in the *trans* C═C bond between both FAs. Nevertheless, there was some specificity for the *trans*-9 C18:1 FA, determined by predicting the *trans*-9 C18:1/*trans*-MUFA abundance ratio (R^2 = 0.64). The latter was further supported by the fact that the most important regression coefficients in the *trans*-9 C18:1/*trans*-MUFA abundance ratio model were near 2871, 2837, 3001, 1446, 1540, 1457, 1251, 1260, 919, 952, 823, 1019, and 1112 cm^{-1} (listed in order of decreasing regression coefficient), and no important variables in the vicinity of 1673 cm^{-1}, which is dominated by the scattering signal from the higher abundance *trans*-10 and *trans*-11 C18:1 FAs, were present (Figure 8).

CLA versus *trans*-MUFA Differentiation. Countries have increased interest in regulating access of *trans*-MUFA to consumers, while some manufacturers aim at increasing beneficial FAs to support health claims on their products. Milk is a major source of dietary *trans* MUFA and CLA as compared to non-ruminant products; thus, determination of the individual quantities of these FAs in milk fat is of importance.

Although the current range of CLA FAs is narrower as compared to previous reports, CLA predictions were satisfactory.[20,31] Results indicated that PLS predictions for rumenic acid relied mostly on the scattering signal near the 1653 cm^{-1} peak, while the *trans*-MUFA

group was concentrated in the vicinity of 1674 cm^{-1}. This specificity and the very good predictions for the CLA and the *trans*-MUFAs allow Raman spectroscopy to emerge as an ideal candidate for simultaneous quantification and differentiation between the less desired TFAs (with the exception of vaccenic acid) and carcinogen fighting *cis*-9,*trans*-11 CLA.

Raman Spectroscopy Feasibility. The present paper confirmed previous reports on total CLA determination using Fourier transform Raman spectroscopy and demonstrated that this technique could already be used to address direct semiroutine applications for the quantification of several individual CLA and *trans*-MUFAs. Although Raman spectra of pure *trans*-MUFA standards analyzed at RT and at FT conditions indicated that lack of specificity might be a drawback when it comes to FAs with very similar structural features, specific differentiation between *trans*-MUFAs based on near, mid, or far *trans* C═C bond location might be possible. While a novel level of crystallization using *trans*-MUFAs standards was revealed and temperature-regulating equipment for further investigation of the optimal environmental conditions for analysis of milk fat samples is required, Raman spectra collected at different temperatures are of interest to determine low concentrations of *trans*-unsaturated FAs in milk fat.

AUTHOR INFORMATION

Corresponding Author

*Tel: +32 9 264 90 01. Fax: +32 9 264 90 99. E-mail: Veerle.Fievez@UGent.be.

Funding Sources

The Ph.D. research of I.S. is supported by the Institute for the Promotion of Innovation by Science and Technology in Flanders (IWT), IWT-PhD-project: 60704. B.V. is a postdoctoral fellow of the Fund for Scientific Research-Flanders (Belgium). Analyses on Raman spectroscopy as reported were obtained in collaboration with researchers of the Walloon Agricultural Research Centre, Valorisation of Agricultural Products Department (head: Dr. Pierre Dardenne), within the framework of the collaborative agreement between Lanupro and the Valorization of Agricultural Products Department (A08-TT-0384).

REFERENCES

(1) Risérus, U.; Basu, S.; Jovinge, S.; Fredrikson, G. N.; Ärnlöv, J.; Vessby, B. Supplementation with conjugated linoleic acid causes isomer-dependent oxidative stress and elevated C-Reactive protein. *Am. Heart Assoc. Monogr.* **2002**, *106*, 1925–1929.

(2) Tricon, S.; Burdge, G. C.; Kew, S.; Banerjee, T.; Russell, J. J.; Jones, E. L.; Grimble, R. F.; Williams, C. M.; Yaqoob, P.; Calder, P. C. Opposing effects of *cis*-9, *trans*-11 and *trans*-10, *cis*-12 conjugated linoleic acid on blood lipids in healthy humans. *Am. J. Clin. Nutr.* **2004**, *80*, 614–620.

(3) Loor, J. J.; Lin, X.; Herbein, J. H. Dietary *trans*-vaccenic acid (*trans*11−18:1) increases concentration of *cis*9,*trans*ll-conjugated linoleic acid (rumenic acid) in tissues of lactating mice and suckling pups. *Reprod., Nutr., Dev.* **2002**, *42*, 85–99.

(4) Kuhnt, K.; Kraft, J.; Moeckel, P.; Jahreis, G. *Trans*-11−18:1 is effectively Delta9-desaturated compared with *trans*-12−18:1 in humans. *Br. J. Nutr.* **2006**, *95*, 752–761.

(5) Wang, Y.; Lu, J.; Ruth, M. R.; Goruk, S. D.; Reaney, M. J.; Glimm, D. R.; Vine, D. F.; Field, C. J.; Proctor, S. D. *Trans*-11 vaccenic acid dietary supplementation induces hypolipidemic effects in JCR:LA-*cp* rats. *J. Nutr.* **2008**, *138*, 2117–2122.

(6) Stender, S.; Dyerberg, J. Ã.; Bysted, A.; Leth, T.; Astrup, A. A *trans* world journey. *Atheroscler. Suppl.* **2006**, *7*, 47–52.

(7) Stender, S.; Dyerberg, J. Influence of *trans* fatty acids on health. *Ann. Nutr. Metab.* **2004**, *48*, 61–66.

(8) Food and Drug Regulations, C.R.C. *Food and Drug Acts*; Canada, 2009; c. 870, s.B.01.001.

(9) EFSA Panel on Dietetic Products, Nutrition and Allergies (NDA). Opinion of the scientific panel on dietetic products, nutrition and allergies related to the presence of *trans* fatty acids in foods and the effect on human health of the consumption of *trans* fatty acids. *EFSA J.* **2004**, *81*, 1−49.

(10) Murphy, J. J.; Stanton, C.; O'Donovan, M.; Kavanagh, S.; Maher, J.; Patton, J.; Mohammed, R. Adding value to milk by increasing its protein and CLA contents. *Teagasc Agriculture and Food Development Authority*; Oak Park, Carlow, Ireland, 2008; http://www.teagasc.ie/research/reports/dairyproduction/5400/eopr-5400.pdf.

(11) Murphy, J. J.; Coakley, M.; Stanton, C. Supplementation of dairy cows with a fish oil containing supplement and sunflower oil to increase the CLA content of milk produced at pasture. *Livest. Sci.* **2008**, *116*, 332–337.

(12) Belton, P. S.; Wilson, R. H.; Sadeghi-Jorabchi, H.; Peers, K. E. A rapid method for the estimation of isolated *trans* double bonds in oils and fats using FTIR combined with ATR. *Lebensm.-Wiss. Technol.* **1988**, *21*, 153–157.

(13) Lanser, A.; Emken, E. Comparison of FTIR and capillary gas chromatographic methods for quantitation of *trans* unsaturation of fatty acid methyl esters. *J. Am. Oil Chem. Soc.* **1988**, *65*, 1483–1487.

(14) Sleeter, R.; Matlock, M. Automated quantitative analysis of isolated (non conjugated) *trans* isomers using Fourier transform infrared spectroscopy incorporating improvements in the procedure. *J. Am. Oil Chem. Soc.* **1989**, *66*, 121–127.

(15) Kramer, J. K. G.; Fellner, V.; Dugan, M.; Sauer, F.; Mossoba, M.; Yurawecz, M. Evaluating acid and base catalysts in the methylation of milk and rumen fatty acids with a special emphasis on conjugated dienes and total *trans* fatty acids. *Lipids* **1997**, *32*, 1219–1228.

(16) Mossoba, M.; Milosevic, V.; Milosevic, M.; Kramer, J. K. G.; Azizian, H. Determination of total *trans* fats and oils by infrared spectroscopy for regulatory compliance. *Anal. Bioanal. Chem.* **2007**, *389*, 87–92.

(17) Mossoba, M.; Adam, M.; Lee, T. Rapid determination of total *trans* fat content − An attenuated total reflection infrared spectroscopy international collaborative study. *J. AOAC Int.* **2001**, *84*, 1144–1150.

(18) Adam, M.; Mossoba, M. M.; Lee, T. Rapid determination of total *trans* fat content by attenuated total reflection infrared spectroscopy: An international collaborative study. *J. Am. Oil Chem. Soc.* **2000**, *77*, 457–462.

(19) Juanéda, P.; Ledoux, M.; Sébédio, J. L. Analytical methods for determination of *trans* fatty acid content in food. *Eur. J. Lipid Sci. Technol.* **2007**, *109*, 901–917.

(20) Meurens, M.; Baeten, V.; Yan, S. H.; Mignolet, E.; Larondelle, Y. Determination of the conjugated linoleic acids in cow milk fat by Fourier transform Raman spectroscopy. *J. Agric. Food Chem.* **2005**, *53*, 5831–5835.

(21) Stefanov, I.; Baeten, V.; Abbas, O.; Colman, E.; Vlaeminck, B.; De Baets, B.; Fievez, V. Analysis of milk odd- and branched-chain fatty acids using FT-Raman spectroscopy. *J. Agric. Food Chem.* **2010**, *58*, 10804–10811.

(22) Scheerlinck, K.; De Baets, B.; Stefanov, I.; Fievez, V. Subset Selection from multi-experiment data sets with application to milk fatty acid profiles. *Comput. Electron. Agric.* **2010**, *73*, 200–212.

(23) Stefanov, I.; Vlaeminck, B; Fievez, V. A novel procedure for routine milk fat extraction based on dichloromethane. *J. Food Compos. Anal.* **2010**, *23*, 852–855.

(24) Svein, A. Identification of fatty acids in gas chromatography by application of different temperature and pressure programs on a single capillary column. *J. Chromatogr., A* **2003**, *1015*, 151–161.

(25) Kramer, J.; Hernandez, M.; Cruz-Hernandez, C.; Kraft, J.; Dugan, M. Combining results of two GC separations partly achieves determination of all *cis* and *trans* 16:1, 18:1, 18:2 and 18:3 except CLA isomers of milk fat as demonstrated using Ag-Ion SPE fractioning. *Lipids* **2008**, *43*, 259–273.

(26) Martin, C. A.; de Oliveira, C. C.; Visentainer, J. V.; Matsushita, M.; de Souza, N. E. Optimization of the selectivity of a cyanopropyl stationary phase for the gas chromatographic analysis of *trans* fatty acids. *J. Chromatogr., A* **2008**, *1194*, 111–117.

(27) Vlaeminck, B.; Dufour, C.; Van Vuuren, A. M.; Cabrita, A. M. R.; Dewhurst, R. J.; Demeyer, D.; Fievez, V. Potential of odd and branched chain fatty acids as microbial markers: Evaluation in rumen contents and milk. *J. Dairy Sci.* **2005**, *88*, 1031–1041.

(28) Abbas, O.; Fernandez Pierna, J. A.; Codony, R.; Von Holst, C.; Baeten, V. Assessment of the discrimination of animal fat by FT-Raman spectroscopy. *J. Mol. Struct.* **2009**, *924—926*, 294–300.

(29) Reynolds, C. M.; Loscher, C. E.; Moloney, A. P.; Roche, H. M. *Cis*-9, *trans*-11-conjugated linoleic acid but not its precursor *trans*-vaccenic acid attenuate inflammatory markers in the human colonic epithelial cell line Caco-2. *Br. J. Nutr.* **2008**, *100*, 13–17.

(30) Anadon, A.; Martinez-Larranaga, M. R.; Martinez, M. A.; Ares, I.; Ramos, E.; Gomez-Cortes, P.; Juarez, M. Miguel A. De la Fuente. Acute oral safety study of dairy fat rich in *trans*-10 C18:1 versus vaccenic plus conjugated linoleic acid in rats. *Food Chem. Toxicol.* **2010**, *48*, 591–598.

(31) Bernuy, B.; Meurens, M.; Mignolet, E.; Larondelle, Y. Performance comparison of UV and FT-Raman spectroscopy in the determination of conjugated linoleic acids in cow milk fat. *J. Agric. Food Chem.* **2008**, *56*, 1159–1163.